JOURNAL OF GEOPHYSICAL RESEARCH, VOL. 102, NO. D22, PAGES 25,797–25,806, NOVEMBER 27, 1997

Principal modes of the total ozone on the Southern Oscillation timescale and related temperature variations

Mary T. Kayano

Instituto Nacional de Pesquisas Espaciais, São José dos Campos, Brazil

Abstract. Total ozone and associated temperature variations on the Southern Oscillation timescale have been investigated using monthly total ozone mapping spectrometer and temperature data for the latitudinal domain between 70°N and 70°S and from 1979 to 1991. The first two modes for total ozone describe the anomalous total ozone patterns associated with the extremes in the Southern Oscillation. The first mode has the largest loadings in the southern hemisphere (SH) subtropics and midlatitudes with an east-west dipole in antiphase with a tropical east-west dipole. The second mode has its largest loadings in the tropics with an east-west dipolar pattern. These modes are intimately related to variations in the mean temperature in the lower stratosphere, and this relation is such that the total ozone and mean temperature anomalies are positively correlated. The tropospheric temperature patterns are confined in the tropics, where temperature and total ozone anomalies are negatively correlated. The tropical temperature and total ozone variations are driven by modulations in the tropical convection associated with the Southern Oscillation. The Southern Oscillation signals in the stratospheric temperature and in the total ozone are strongest in the SH midlatitudes during the winter-spring period and precede the extremes in the Southern Oscillation Index (SOI) by a few months. Thus the total ozone index, defined similarly to the SOI, seems to be more appropriate than the SOI to monitor the stratospheric temperature in the extratropics, in particular in the SH middle to high latitudes.

1. Introduction

Total ozone with high spatial resolution and nearly global coverage has been measured since October 1978 by the total ozone mapping spectrometer (TOMS) instrument carried on board the Nimbus 7 satellite [*Bowman and Krueger*, 1985; *Bowman*, 1989]. Because of the temporal and spatial homogeneity of this TOMS data set, several aspects of the total ozone long-term variations have been better documented. On the basis of these data, *Bowman* [1989] provided a detailed analysis of the quasi-biennial oscillation (QBO) in the total ozone. He showed that the interannual variability of the total ozone near the equator is dominated by the QBO and that the equatorial total ozone anomalies are negatively correlated with those at middle and high latitudes, particularly during the winter seasons of each hemisphere.

At the equatorial latitudes the dynamical coupling between interannual ozone variations and the QBO-related lower stratospheric zonal wind and temperature variations was previously noted by several authors using ground-based observations [e.g., *Angell and Korshover*, 1973; *Hasebe*, 1980; *Bojkov*, 1987] or satellite observations [e.g., *Hilsenrath and Schlesinger*, 1981; *Tolson*, 1981]. For the QBO timescale the total ozone and lower stratospheric temperature anomalies over the equator are positively correlated [e.g., *Lait et al.*, 1989; *Chandra and Stolarski*, 1991]. Positive correlations between temperature in the lower stratosphere and the total ozone have also been observed in the extratropics on an interannual timescale [e.g., *Labitzke and van Loon*, 1992].

Paper number 97JD02362.
0148-0227/97/97JD-02362$09.00

Besides the QBO, strong El Niño (or Pacific warm) episodes have been proposed to explain anomalous total ozone departures [*Zerefos et al.*, 1982; *Angell*, 1981, 1990; *Bojkov*, 1987; *Komhyr et al.*, 1988]. *Bojkov* [1987] was the first to promulgate a connection between ozone variations and El Niño, according to which, strong El Niño episodes are followed by low total ozone values in the middle and polar latitudes, within a few months time lag. Since El Niño refers to one of the extremes in the Southern Oscillation, opposite variations in the total ozone related to La Niña (or Pacific cold) episodes would be expected.

Indeed, recent findings have provided evidences that the total ozone fields contain variability on the Southern Oscillation timescale [*Shiotani*, 1992; *Zerefos et al.*, 1992; *Hasebe*, 1993; *Randel and Cobb*, 1994; *Stephenson and Royer*, 1995]. *Shiotani* [1992] showed that the Southern Oscillation signal in the total ozone manifests in its asymmetric part, obtained by removing the zonal means, what effectively eliminates most of the QBO signal in the data. In the tropics the Southern Oscillation structure in the total ozone features an east-west anomalous dipole, with a nodal longitude near the dateline [e.g., *Shiotani*, 1992; *Stephenson and Royer*, 1995]. For the El Niño periods the dipole is such that negative total ozone anomalies are associated with enhanced convection in the eastern tropical Pacific and positive anomalies are associated with reduced convection over Indonesia. La Niña episodes feature reversed total ozone anomaly patterns.

Variations in the tropopause height explain a large portion of the spatial and temporal variability of the total ozone through a negative correlation between the total ozone column and the tropopause height [*Schubert and Munteanu*, 1988; *Hasebe*, 1993]. Thus the Southern Oscillation-related anoma-

lous total ozone patterns reflect the variations of the tropopause height caused by changes in the tropical convection [e.g., *Shiotani*, 1992; *Stephenson and Royer*, 1995]. In this regard, *Hasebe* [1993] proposed a mechanistic coupling between sea surface temperature (SST) and total ozone variations, such that SST variations lead to changes in the tropopause height and the vertical ozone advection through modulation of the tropospheric diabatic heating.

In addition, *Randel and Cobb* [1994] showed that the total ozone variability on the Southern Oscillation timescale extends beyond the tropics. For separate analyses of the TOMS data for northern hemisphere (NH) and SH winter-spring periods they found a strong north-south anomalous dipolar structure in the Pacific region, with the largest amplitudes in the winter hemisphere. In agreement, the map of correlation between interannual anomalies of the asymmetric part of the TOMS data and the low-pass-filtered sea level pressure (SLP) at Darwin as presented by *Stephenson and Royer* [1995] gives some indications of the existence of an east-west dipole in the SH midlatitudes in antiphase with a well-defined east-west dipole in the tropics.

The purpose of this paper is to understand better the dynamics of the ozone variations on the Southern Oscillation timescale. The Southern Oscillation-related total ozone patterns and the associated tropospheric and stratospheric temperature patterns are investigated in detail. Since the focus of this paper is on the Southern Oscillation timescale, only the asymmetric part of the fields is examined. The dominant patterns for the TOMS data are determined through empirical orthogonal function (EOF) analysis. Although T. Ambrizzi et al. (A comparison of global tropospheric teleconnections using observed satellite and general circulation model total ozone column data for 1979–91, submitted to *Climate Dynamics*, 1996) have determined the Southern Oscillation-related principal EOF modes for the TOMS data, they limited their discussion to the first mode, and no reference to temperature patterns has been made. So, the present paper intends, in particular, to deepen the knowledge of the ozone-temperature relationships.

2. Data

The ozone data used in this study consist of the monthly TOMS data provided by the National Space Science Data Center. Version 6 of the retrieval algorithm has been used to remove instrumental drift [*Herman et al.*, 1991]. The monthly values are on a grid with a 2.5° in longitude and 2.0° in latitude resolution. For details on the TOMS data the reader is referred to *Bowman and Krueger* [1985] and *Bowman* [1989].

Temperature data have been obtained from the National Centers for Environmental Predictions (NCEP) and were derived from the reanalyzed gridded data produced by the Climate Data Assimilation System (CDAS)/Reanalysis Project [*Kalnay et al.*, 1996]. This data set consists of monthly temperatures at 17 standard pressure levels (1000, 925, 850, 700, 600, 500, 400, 300, 250, 200, 150, 100, 70, 50, 30, 20, and 10 hPa) on a grid with a 2.5° in latitude and longitude resolution.

The absence of inhomogeneities in both data sets makes them highly useful for the study of the low-frequency oscillations and their spatial patterns. Both data sets span from January 1979 through December 1991. For this period the SOI time series provided by NCEP has been used for additional correlation analyses. The SOI is based on observed SLP time series for Tahiti and Darwin, and the procedure for its calculation is described by *Chelliah* [1990].

3. Analysis Procedures

As given by *Shiotani* [1992], zonal means have been removed from the original databases, thus only the asymmetric part of the fields is analyzed. The total ozone and temperature asymmetric time series (hereafter the word "asymmetric" will be omitted) are then sampled for every other gridpoint. Thus the horizontal resolution is reduced to 4° in latitude and 5° in longitude for the TOMS data and to 5° in latitude and longitude for the temperature data. The data are deseasonalized using the 1979–1991 climatology. The anomalous data are treated with a Lanczos low-pass filter with 11 weights and a specified response of 0.5 at 12 months, yielding a filtered time series from June 1979 through July 1991. This filter effectively eliminates high-frequency oscillations with periods of less than 8 months [*Trenberth*, 1984] and is the same as that used by *Stephenson and Royer* [1995] in their study of the low-frequency variability in the total ozone.

The above procedures have been performed for total ozone, for temperature at every standard pressure level, and for mean temperature ($[T]$) for selected layers. Five separate layers (1000–850, 600–400, 300–200, 150–70, and 30–10 hPa) are chosen to represent the lower, middle, and upper troposphere and lower and middle stratosphere. The mean temperature is calculated using the available data for the layer. The domain of the study is limited between 70°N and 70°S.

The principal EOF modes for the total ozone are determined using the correlation matrix. The principal component (PC) time series (amplitude time series of the EOF modes) are analyzed to investigate the interannual variability of each pattern. The PC time series are also used to determine the associated $[T]$ patterns. For a certain mode and a certain layer the map of simultaneous correlations between PC time series and the filtered anomalous $[T]$ time series for every gridpoint results in the associated $[T]$ patterns.

The evolving aspects of the total ozone patterns are examined through lagged correlation maps, which are constructed by correlating filtered SOI and filtered anomalous total ozone time series. Similarly, $[T]$ correlation maps are constructed for the lower stratosphere. The calculations are made from -6 to $+6$ month lags for every 1 month lag, with positive lag meaning that the SOI time series precede the total ozone or $[T]$ time series. Following *Stephenson and Royer* [1995], 13 degrees of freedom are assumed for 13 years of data. Using the Student's t test, it is found that correlations >0.47 are significant at the 90% level of significance. Only correlations >0.5 are considered in this analysis.

4. Results

4.1. Total Ozone Patterns

The first mode explains 17.3% of the total interannual variance of the TOMS data and has its largest loadings in the SH subtropics and midlatitudes featuring a strong east-west dipole (Figure 1a). Loadings of -0.8 centered at 45°S in the southeastern Pacific and of $+0.8$ at 50°S in the south Indian Ocean indicate that this mode accounts for 64% of the total interannual variance in these regions. It is also noted that a tropical east-west dipole exists in antiphase to the SH dipole, both having nodal longitudes approximately at 140°E.

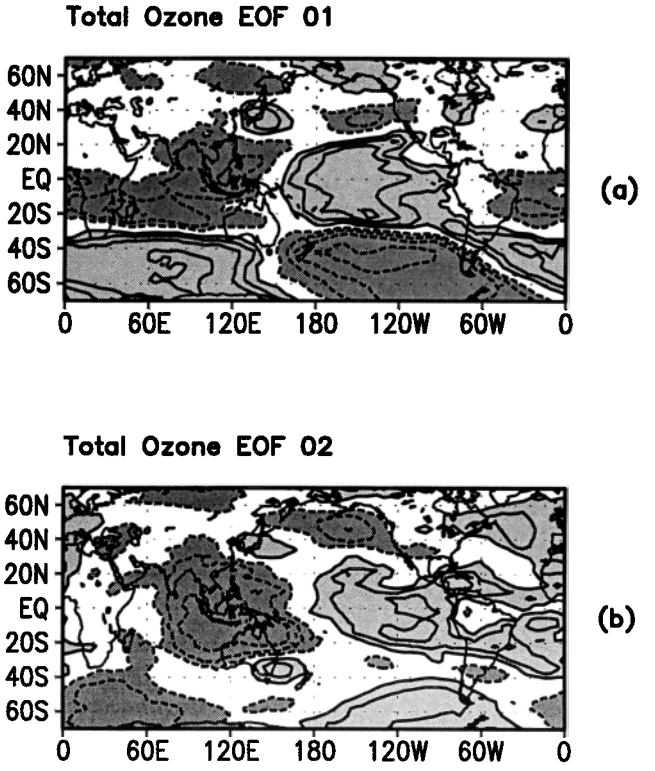

Figure 1. The empirical orthogonal function (EOF) patterns for the low-pass-filtered asymmetric part of the total ozone corresponding to (a) the first mode and (b) the second mode. The contour interval is 0.2, and the zero line has been omitted. The loadings are contoured with positive (negative) values indicated by solid (dashed) lines. Light (dark) shading indicates values greater (less) than 0.2 (−0.2).

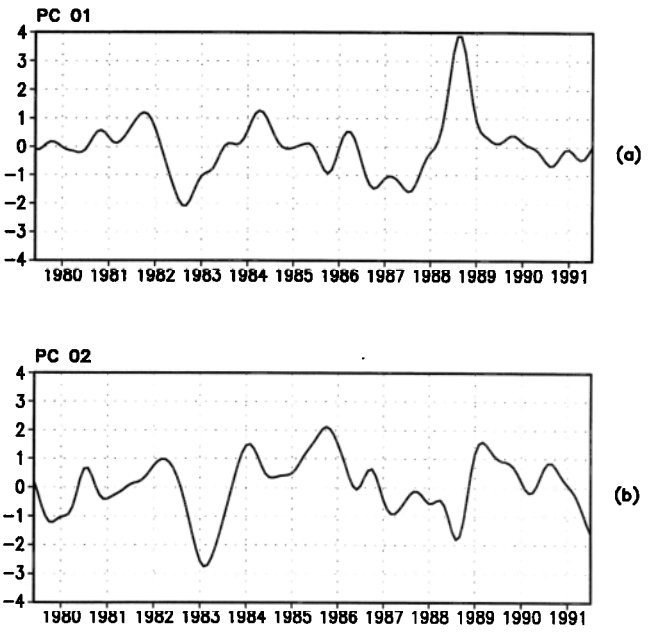

Figure 2. The amplitude time series associated with the patterns shown in Figure 1 for (a) the first mode (PC 01) and (b) the second mode (PC 02).

The first mode contains anomalous ozone patterns previously found to be associated with extremes in the Southern Oscillation. For negative amplitudes of this mode (Figure 2a), which correspond to El Niño periods (1982–1983 and 1986–1987), negative total ozone anomalies are found over the tropical central and eastern Pacific, the subtropical South Atlantic, and the areas south of 40°S in the Indian Ocean. Positive total ozone anomalies are found over the tropical Indian and western Pacific Oceans, the tropical Atlantic, and the areas south of 40°S in the southern Pacific. Reversed patterns are observed for positive amplitudes (Figures 1a and 2a), which correspond to La Niña episodes (1984 and 1988–1989). The relationship between the Southern Oscillation and the anomalous total ozone patterns in the tropics, as shown in previous works, is explained by variations in the tropopause height caused by the anomalous tropical convection [e.g., *Shiotani*, 1992; *Randel and Cobb*, 1994]. Figure 1a shows that the ozone anomalies in the tropics are negatively correlated with those in SH midlatitudes, in agreement with the results achieved by *Randel and Cobb* [1994] for the July–November period.

The second mode, which explains 10.5% of the total interannual variance of the TOMS data, has its largest loadings in the tropics (Figure 1b). For negative amplitudes of this mode, negative total ozone anomalies are observed over the central and eastern Pacific, the central South America, and most of the tropical Atlantic; positive anomalies are found over the Indian and western Pacific Oceans (Figures 1b and 2b). The patterns are reversed for the case of positive amplitudes. The PC time series for the second mode indicates that it describes the anomalous features in the total ozone associated with the extremes in the Southern Oscillation.

Although both modes have links with the Southern Oscillation, they describe slightly different aspects of the total ozone anomaly field. Indeed, the two main peaks in first mode PC time series (September 1982 and September 1988) occur a few months before the extremes in the Southern Oscillation (1982–1983 El Niño and 1988–1989 La Niña). The corresponding two peaks in the second mode PC time series (one main peak in early 1983 and a secondary peak in early 1989) coincide with peaks in the SOI time series. Thus, in terms of the ozone variations associated with the Southern Oscillation, it is noticed that the first mode relates to the initial stages of the El Niño and La Niña phenomena, while the second mode relates to their mature stages.

4.2. Temperature Patterns

Figure 3 illustrates the $[T]$ patterns associated with the first mode for five layers. The largest $[T]$ correlations for the lower and middle troposphere are found mostly in the tropics; for the upper troposphere they are observed in the tropics and SH midlatitudes. From Figures 1a and 3 one can see that the total ozone and the tropospheric $[T]$ anomalies are negatively correlated in the tropics and positively correlated in the SH midlatitudes. The lower stratospheric $[T]$ patterns are, overall, similar to the total ozone first-mode patterns, with the total ozone and $[T]$ anomalies being positively correlated everywhere. At middle stratosphere, significant correlations are found only in the SH subtropics and midlatitudes, where total ozone and $[T]$ anomalies are positively correlated.

The $[T]$ patterns associated with the second mode at the five separate layers are presented in Figure 4. The $[T]$ patterns at the two lower tropospheric layers exhibit much more horizontal structure than those associated with the first mode. At the

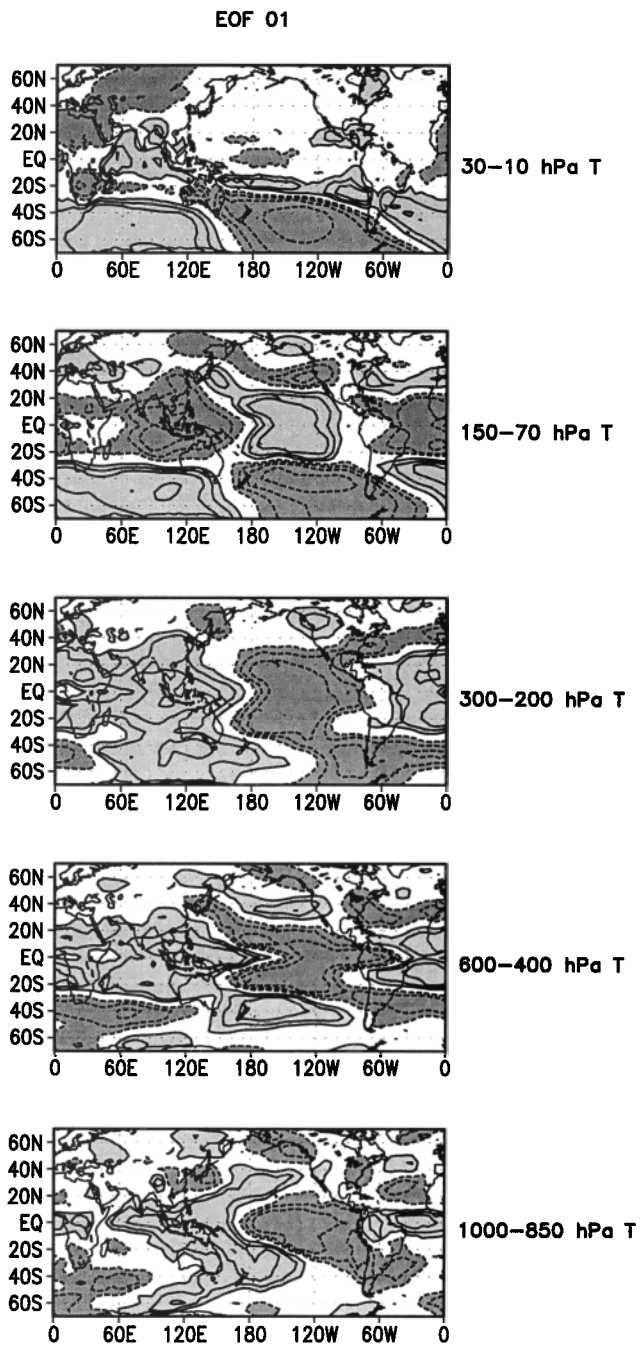

Figure 3. The mean temperature patterns associated with the first total ozone EOF mode for the five layers: 30–10, 150–70, 300–200, 600–400, and 1000–850 hPa. The contour interval is 0.2, and the zero line has been omitted. The correlations are contoured with positive (negative) values indicated by solid (dashed) lines. Light (dark) shading indicates correlations greater (less) than 0.2 (−0.2). For details on the procedures used to get these correlations the reader is referred to the text.

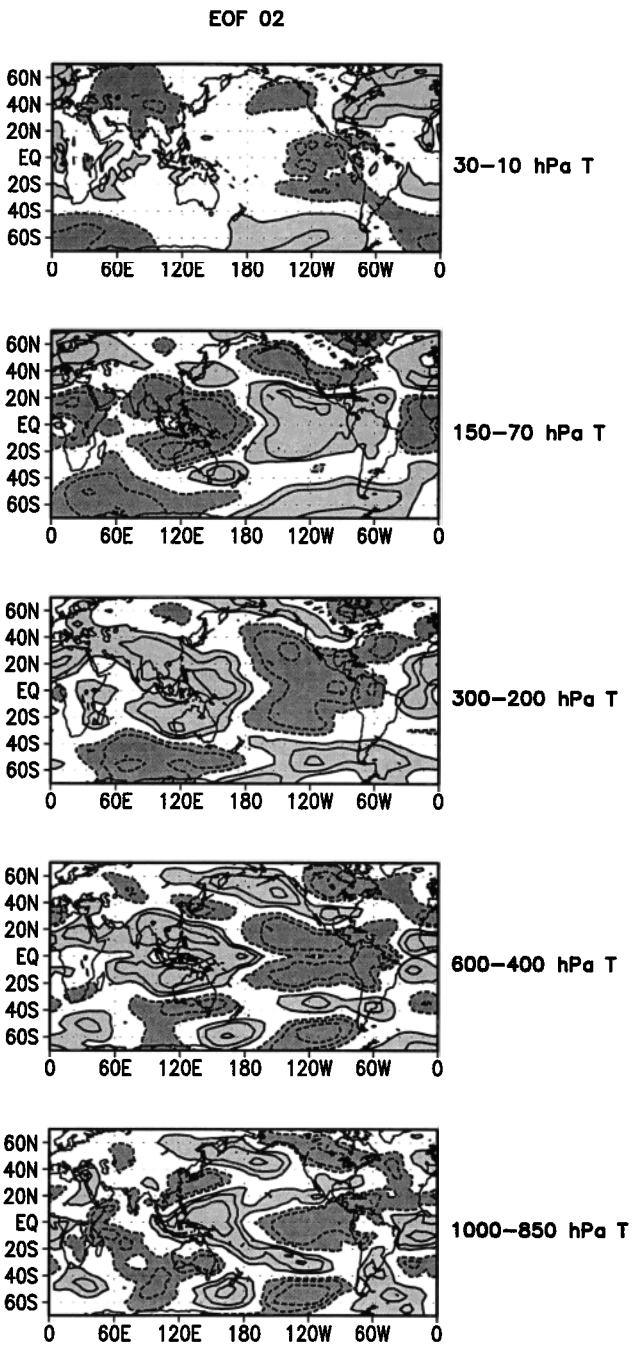

Figure 4. Same as Figure 3 except associated with the second total ozone EOF mode.

middle stratosphere, no significant correlations are observed for the second mode. Analogous to the first mode, the $[T]$ patterns at the lower stratosphere are quite similar to the total ozone patterns.

In summary, significant correlations in the troposphere are mostly confined in the tropics, where $[T]$ and total ozone anomalies are negatively correlated. The total ozone patterns have remarkable similarities with the associated $[T]$ patterns at the lower stratosphere, and $[T]$ anomalies in this layer are positively correlated with the total ozone anomalies.

4.3. Vertical Temperature Structure

Figures 5a and 5b show the vertical cross sections of the filtered temperature anomalies at some reference latitudes (45°S and equator, where the first mode's largest loadings are centered) and for the months corresponding to the main peaks in the PC time series of the first mode. These peaks occur in

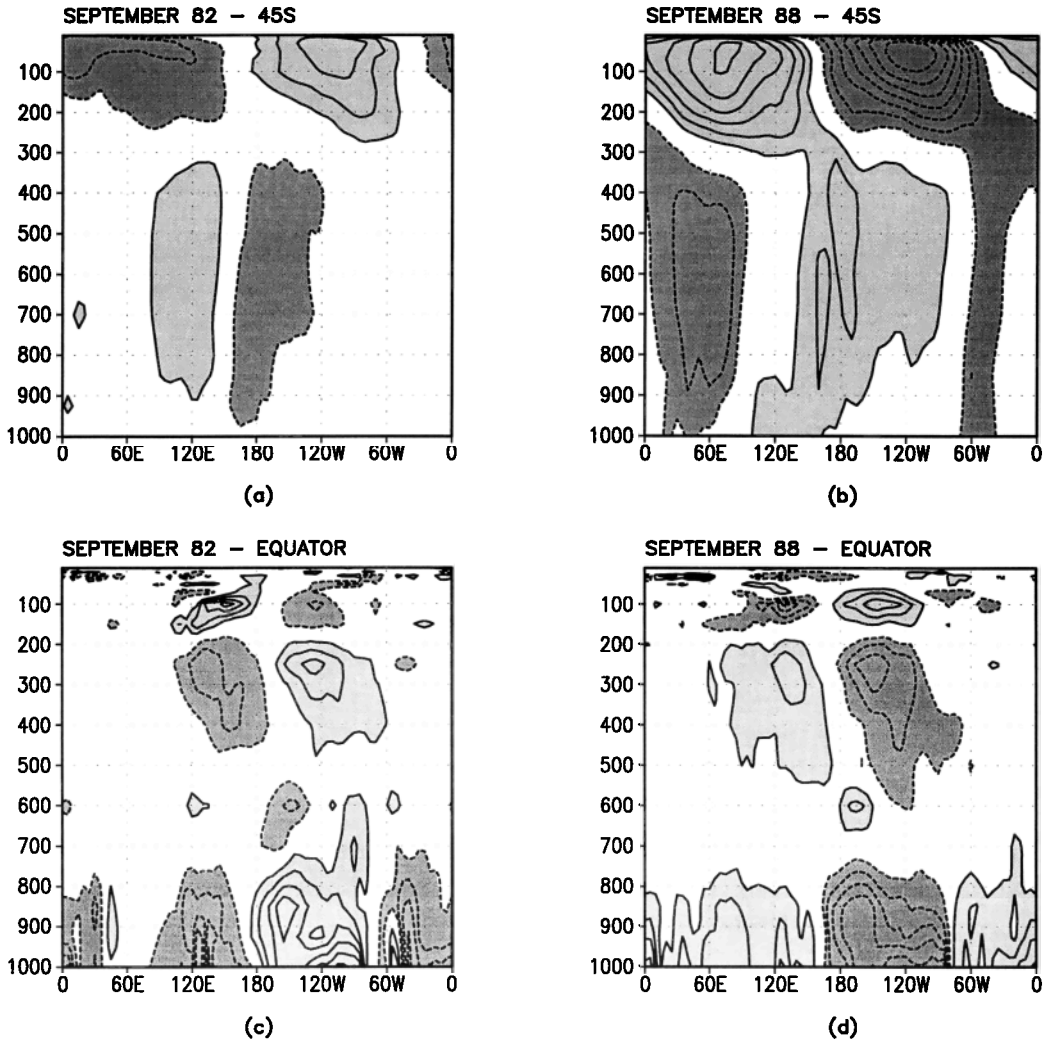

Figure 5. Vertical cross section of the asymmetric temperature anomalies at (a) 45°S for September 1982, (b) 45°S for September 1988, (c) the equator for September 1982, and (d) the equator for September 1988. The contour interval is 4°C for Figures 5a and 5b and 2°C for Figures 5c and 5d. The zero line has been omitted. Positive (negative) anomalies are contoured with solid (dashed) lines. Light (dark) shading indicates values greater (less) than 4°C (−4°C) in Figures 5a and 5b and greater (less) than 2°C (−2°C) in Figures 5c and 5d.

September 1982 (early El Niño) and September 1988 (early La Niña).

Figure 5a illustrates the vertical cross section at 45°S for September 1982, a month of the strong 1982–1983 El Niño onset. There is an east-west dipole extending throughout the upper troposphere and stratosphere, with centers at 60°E (central value of −8°C) and at 120°W (central value of 12°C). The anomalies below 300 hPa are quite small, with the extreme values ranging from −4°C to 4°C, centered in the middle troposphere and confined longitudinally over the southeastern Indian and western Pacific Oceans.

Figure 5b shows the vertical cross section at 45°S for September 1988, a month of the early development stage of the 1988–1989 La Niña. As expected, the patterns in this diagram are the reverse of those shown in Figure 5a. However, the magnitudes of the anomalies are, in general, more than double those corresponding to September 1982. This is particularly true for the upper level east-west dipole, which shows the extreme anomalies between −28°C (at 120°W) and 24°C (at 70°E). This dipole has comparable vertical and longitudinal extensions to those of the dipole for September 1982. The anomalies below 300 hPa are also centered in the middle troposphere, with the dipole showing less longitudinal confinement with extreme values of 8°C (centered around the dateline) and −8°C (centered at 60°E).

The temperature anomalies along the equator (Figures 5c and 5d) present distinct vertical structures as compared to the sections at 45°S. Indeed, the anomalies are layer stratified, with the anomalies for September 1982 and September 1988 showing almost the same magnitudes. The anomalies decrease with height, and they occur in the lower troposphere, the upper troposphere, and the lower stratosphere. The relatively weak anomalies at the lower stratosphere are both longitudinal and vertically confined and have opposite signs with respect to the lower layer anomalies.

The largest temperature anomalies at the equator are found

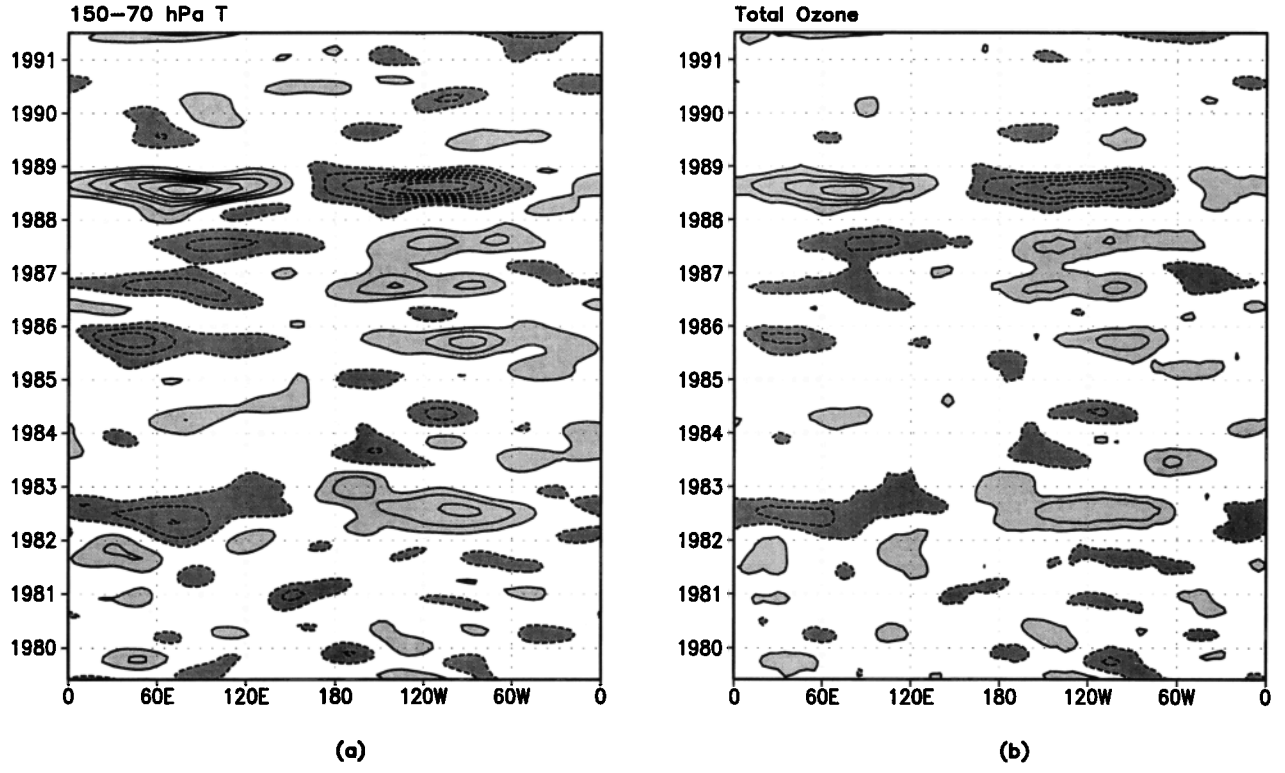

Figure 6. Longitude-time plots for (a) the filtered asymmetric mean temperature in the lower stratosphere anomalies at 45°S and (b) the filtered asymmetric total ozone anomalies at 45°S. The contour interval for the temperature anomalies is 0.4°C and for the ozone anomalies is 4 DU. The zero line has been omitted. Light (dark) shading indicates values greater (less) than 0.4°C (−0.4°C) in Figure 6a and greater (less) than 4 DU (−4 DU) in Figure 6b.

in the lower troposphere and at 45°S in the stratosphere. A possible explanation for the vertically damped signals at the equator and the large stratospheric amplitudes at 45°S is that the Southern Oscillation-related low-frequency interannual variability propagates barotropically out of the tropical troposphere into the winter hemisphere from where it propagates vertically into the stratosphere.

4.4. The Total Ozone and the Lower Stratospheric [*T*] in the SH Midlatitudes

The results above show an important relation between the total ozone and the stratospheric temperature variations on the Southern Oscillation timescale with the signals being stronger in the SH midlatitudes. This relation is now further investigated displaying the filtered total ozone and [*T*] at 150–70 hPa anomalies at 45°S in time versus longitude plots. The presence of synchronous variations in the total ozone and [*T*] at the lower stratosphere at 45°S is clear from Figures 6a and 6b. In both figures the 1988 east-west dipole is considerably stronger compared to those of the other periods of extreme in the Southern Oscillation, such as during 1982–1983 and 1986–1987.

4.5. Indices for the Total Ozone and the Lower Stratospheric [*T*]

Southern Oscillation-related patterns on both total ozone and lower stratospheric [*T*] are conspicuous; this is what renders these variables potential tools for use in monitoring low-frequency variability. So, in analogy to the SOI, indices for total ozone and [*T*] in the lower stratosphere have been established to explore this potentiality. Areas of the largest loadings for the first mode for the TOMS data are represented by equally sized boxes with 10° in latitude and of 20° in longitude. Two boxes centered at (45°S, 150°W), the western box, and (45°S, 70°E), the eastern box, account for the SH midlatitude dipole. Two others centered at the equator line and longitudes of 150°W (the western box) and 110°E (the eastern box) represent the tropical dipole. The mean anomalies of the total ozone and of the lower stratospheric [*T*] are calculated for each box. Indices for total ozone and for [*T*] are defined as the difference of the mean anomalies in the western box minus mean anomalies in the eastern box. The indices are normalized by their standard deviations, so that they can be compared as undimensional numbers.

Figure 7 shows the PC time series for the first mode, the low-pass-filtered SOI, and the indices for the total ozone and [*T*] at 45°S. The total ozone and [*T*] indices at 45°S have a strong and positive correlation with each other and a strong and negative correlation with the first-mode PC time series. The first mode thus describes mostly the SH midlatitude variations in the total ozone, which are dynamically connected with variations in the lower stratospheric temperature. It is apparent that peaks in the total ozone and [*T*] indices at 45°S occur a few months before the peaks in the low-pass-filtered SOI.

Figure 8 shows the PC time series for the second mode, the low-pass-filtered SOI, and the same indices at the equator. The second-mode PC time series resembles the time series of the

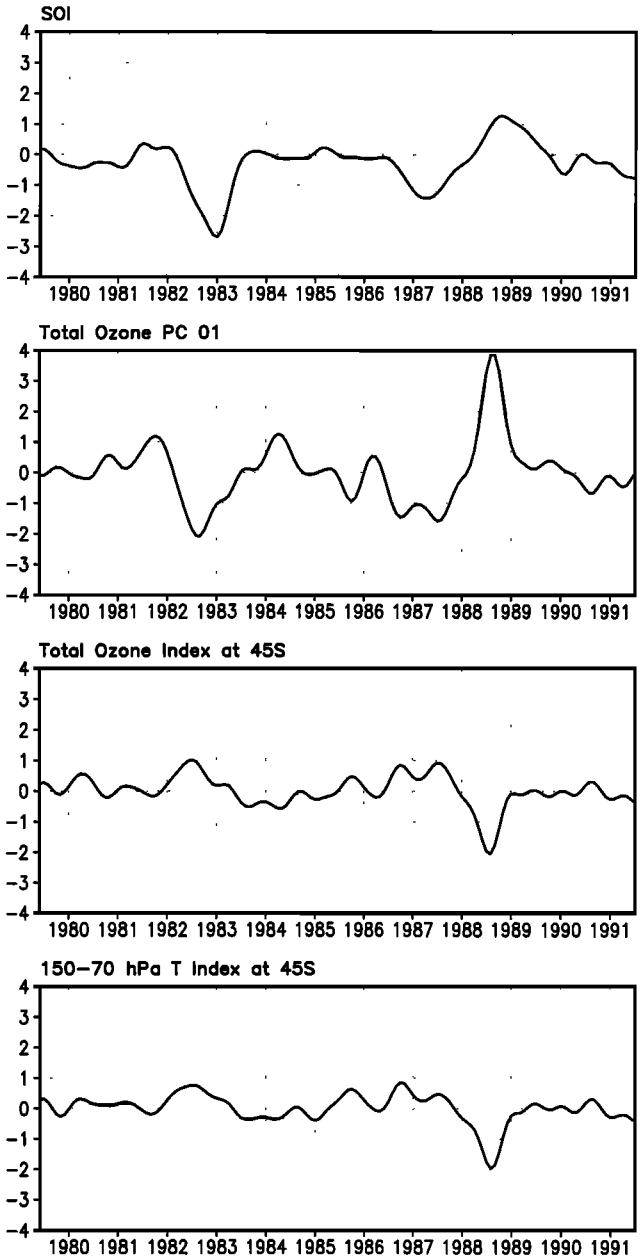

Figure 7. The low-pass-filtered Southern Oscillation Index (SOI), the amplitude time series of the first mode for the total ozone, the low-pass-filtered total ozone index at 45°S, and the low-pass-filtered lower stratospheric [T] index at 45°S.

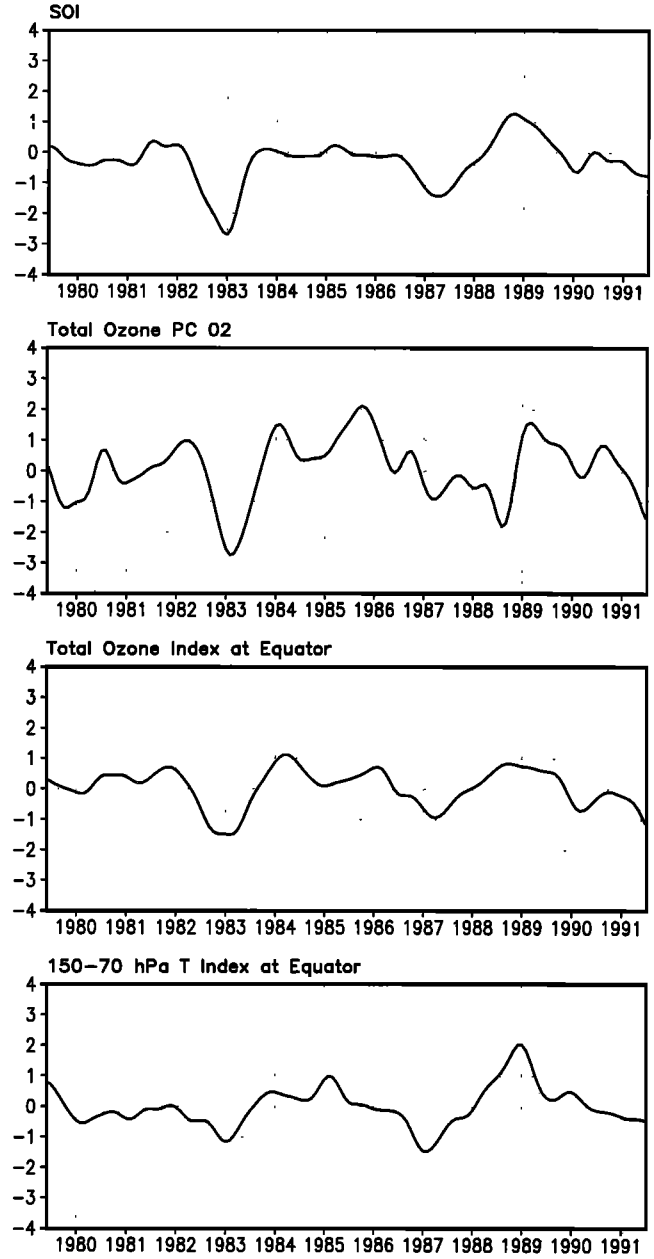

Figure 8. The low-pass-filtered SOI, the amplitude time series of the second mode for the total ozone, the low-pass-filtered total ozone index at the equator, and the low-pass-filtered lower stratospheric [T] index at the equator.

equatorial total ozone index. The equatorial [T] index and SOI time series exhibit coherent fluctuations. Concurrent peaks are noticed in the four plots, particularly during 1982–1983 El Niño and 1988–1989 La Niña episodes. So, the second mode describes mostly the Southern Oscillation-related variations in the total ozone in the tropics.

4.6. Lagged Correlation Maps

The indices at 45°S peaking a few months before the SOI and the quasi-simultaneous occurrence of the peaks in the tropical indices and the SOI indicate different phase relations of the total ozone and the lower tropospheric [T] and SOI for the SH midlatitudes and the tropics. These phase relations are studied using correlation maps, which are constructed by calculating lagged correlations between (1) the filtered SOI and total ozone anomalous time series and (2) the filtered SOI and lower stratospheric [T] anomalous time series. Figures 9 and 10 show the maps for −6, zero, and +6 month lags.

The lag zero patterns (Figure 9) are quite similar to those of *Randel and Cobb* [1994] which were shown to be related to the Southern Oscillation and to those displayed in Figure 1a. However, the SH midlatitude dipole does not have its maximum strength at lag zero. Another interesting aspect is the latitudinal dependence of the temporal evolution of the patterns.

The tropical dipole featuring negative correlations over the Atlantic/African area and positive correlations around the

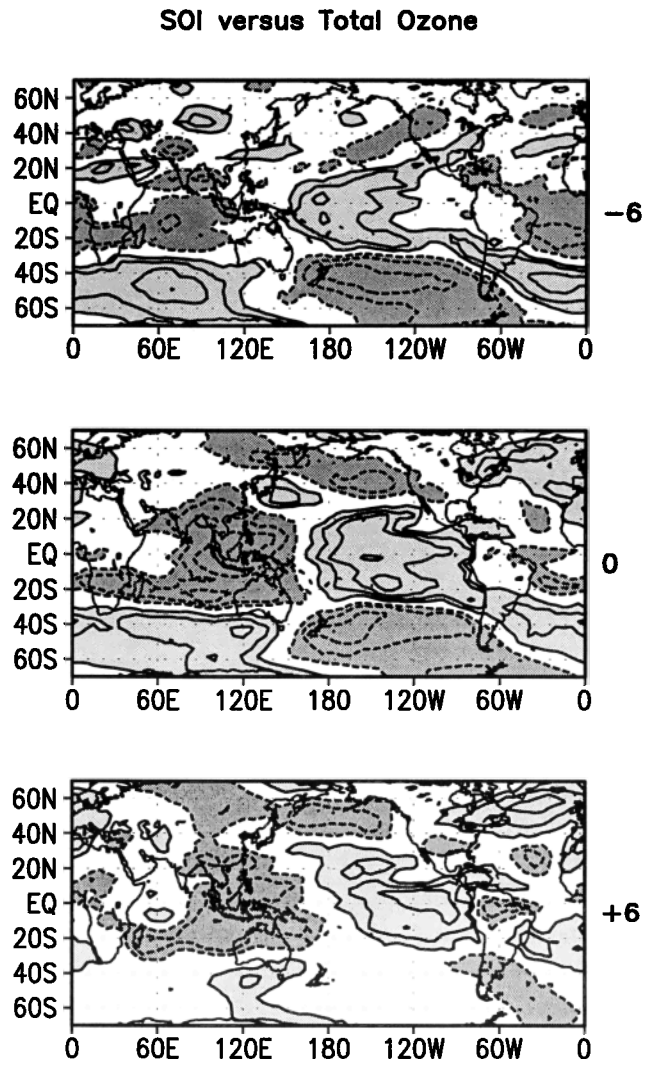

Figure 9. Maps of the lagged correlations between the low-pass-filtered SOI and the low-pass-filtered asymmetric total ozone anomaly time series for −6, zero, and +6 month lags. The contour interval is 0.2, and the zero line has been omitted. The correlations are contoured with positive (negative) values indicated by solid (dashed) lines. Light (dark) shading indicates correlations greater (less) than 0.2 (−0.2).

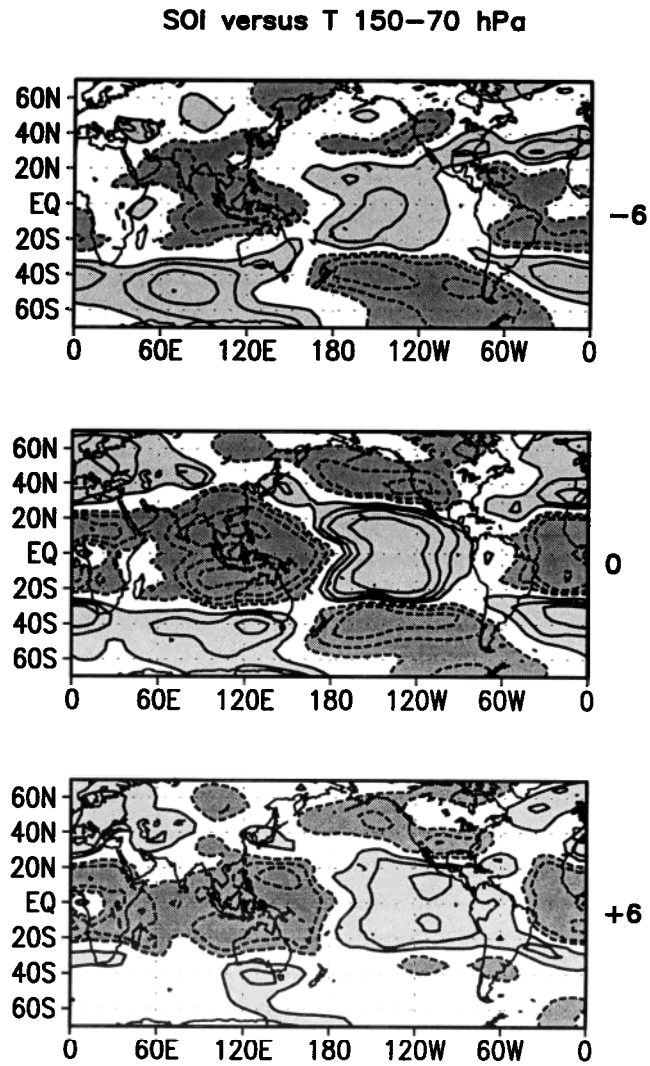

Figure 10. Maps of the lagged correlations between the low-pass-filtered SOI and the low-pass-filtered asymmetric lower stratospheric [T] anomaly time series for −6, zero, and +6 month lags. Display is the same as that used in Figure 9.

dateline at −6 month lag gradually intensifies as it moves eastward and reaches its maximum strength at +3 month lag (not shown in Figure 9). This evolving feature is consistent with the eastward movement of the tropical convection from the western to the central and the eastern Pacific as observed during the El Niño onset. It can be inferred from the correlation maps that variations in the tropical convection are followed within 3 months time lag by variations in the tropical total ozone.

In the NH midlatitudes a weak dipole with positive correlations in the North Atlantic and negative correlations in the eastern North Pacific is observed after the tropical dipole, with its maximum strength occurring at +6 month lag. This result is consistent with the ozone/El Niño relationship put forth by *Bojkov* [1987].

In the SH midlatitudes a strong dipole with centers in the South Pacific and the south Indian Ocean has a strikingly different evolving characteristic. A well-defined dipole observed at −6 month lag remains intense up to −2 month lag (not shown in Fig. 9) and declines rapidly afterward. Therefore the SH midlatitude Southern Oscillation signals in the total ozone precede by 6–2 months the extremes of the SOI.

Examination of Figure 10 indicates a very consistent evolution of lower stratospheric [T] patterns. Coherence between the evolving features of total ozone and [T] patterns makes the results of this paper physically sound.

5. Remarks and Conclusions

Total ozone and associated temperature variations on the Southern Oscillation timescale have been investigated using monthly TOMS and temperature data for the space domain between 70°N and 70°S and the period from 1979 to 1991. The first two modes for total ozone are related to the extremes in the Southern Oscillation. The first mode has the largest loadings in the SH subtropics and midlatitudes, displaying an east-west dipole in antiphase with the tropical east-west dipole. The

second mode has its largest loadings in the tropics with an east-west dipolar pattern. Positively correlated variations are observed for the associated patterns of the mean temperature ($[T]$) in the lower stratosphere. On the other hand, the dominant $[T]$ patterns for the tropospheric layers are confined in the tropics, where the total ozone and $[T]$ anomalies are negatively correlated.

For the tropics the existence of a mechanistic relationship between the Southern Oscillation and the total ozone variations [e.g., *Shiotani*, 1992; *Hasebe*, 1993] is well established. During the extremes in the Southern Oscillation, modulations in the tropical convection induce thermal and dynamical variations in the troposphere, with the tropopause altitude being altered. This happens because in the tropical regions with anomalously enhanced (reduced) convection, the presence (absence) of tropospheric heating by latent heat release and upward (downward) motions push up (down) the tropopause. In the stratosphere, where no release of latent heat takes place, an air parcel moving upward (downward) experiences adiabatic cooling (warming). When the lower stratosphere gets cooler (warmer), the reduction (increase) of the ozone at those levels yields less (more) total ozone.

The SH midlatitude dipoles observed in the first total ozone mode and in the associated lower stratospheric $[T]$ patterns have previously been found to be related to the Southern Oscillation by *Randel and Cobb* [1994]. However, the principal component time series corresponding to the first mode as well as the total ozone and the lower stratospheric $[T]$ indices at 45°S show extreme values during the SH winter-spring (Figure 7). This suggests that in the absence of seasonal circulation effects, as for the QBO anomalies, the photochemistry is responsible for the seasonal modulation of the Southern Oscillation-related total ozone anomalies. Since photochemical lifetimes are longer during winter, the Southern Oscillation-related vertical advection of total ozone in the SH midlatitudes would result in corresponding larger anomalies.

Analyses of the evolution of the Southern Oscillation-related total ozone and the lower stratospheric $[T]$ patterns show coherent features, with a latitudinal dependence for both variables. For the tropics and for the -6 to $+3$ month lags an east-west dipole intensifies as it moves eastward. Therefore variations in the tropical total ozone and in the lower stratospheric $[T]$ follow the Southern Oscillation-related tropical convection changes with a time lag of 3 months. In the NH midlatitudes, there is a weak east-west dipole with centers in the North Atlantic and eastern North Pacific with its maximum amplitude at $+6$ month lag, thus indicating a delayed response of the total ozone and the lower stratospheric $[T]$ to the Southern Oscillation. This result is consistent with the ozone/El Niño relationship proposed by *Bojkov* [1987].

In the SH midlatitudes a strong east-west dipole shows an intensification and eastward movement for negative lags and a pronounced decay for positive lags. The largest correlations are observed from -6 to -2 month lags. Such time lags are also observed comparing the SOI to the indices for the total ozone and the stratospheric $[T]$ at 45°S (Figure 7). Indeed, the largest amplitudes for these indices occur during the SH winter-spring months, while for the SOI they occur during the following SH summer months. As mentioned above, the photochemistry might produce a seasonal modulation of the Southern Oscillation-related total ozone anomalies. In addition, changes in the tropical tropospheric circulation caused by alterations in the SST and the convective activity during the early and developing stages of the El Niño and La Niña episodes propagate barotropically out of the tropics into the winter hemisphere and from there propagate vertically into the stratosphere. This dynamic process favors the production through photochemistry of even larger signals in the SH midlatitude total ozone during the SH winter-spring months.

An important result of this paper is that the total ozone index defined similarly to the SOI seems to be better than the SOI as a climate monitor of the lower stratospheric temperatures in the extratropics, especially in the SH middle to high latitudes. It is, however, worthwhile to recall that only the asymmetric parts of the fields were considered in the analyses. So, the transport mechanisms might play an important role in the Southern Oscillation-related variations in the total ozone and the temperature.

The author is aware that the results of this paper were based on relatively short time series. More conclusive results should stem from analyses based on longer time series.

Acknowledgments. The author was partially supported by Conselho Nacional de Desenvolvimento Científico e Tecnológico under grant 300033/94-0. Thanks are due to M. A. Maringolo Lemes for going through the manuscript. Thanks are due to the anonymous reviewers for helpful comments and suggestions.

References

Angell, J. K., Comparison of variations in atmospheric quantities with sea surface temperature variations in the equatorial eastern Pacific, *Mon. Weather Rev.*, *109*, 230–243, 1981.

Angell, J. K., Influence of equatorial QBO and SST on polar total ozone and the 1990 Antarctic ozone hole, *Geophys. Res. Lett.*, *17*, 1569–1572, 1990.

Angell, J. K., and J. Korshover, Quasi-biennial and long-term fluctuations in total ozone, *Mon. Weather Rev.*, *101*, 426–443, 1973.

Bojkov, R. D., The 1983 and 1985 anomalies in ozone distribution in perspective, *Mon. Weather Rev.*, *115*, 2187–2201, 1987.

Bowman, K. P., Global patterns of the quasi-biennial oscillation in total ozone, *J. Atmos. Sci.*, *46*, 3328–3343, 1989.

Bowman, K. P., and A. J. Krueger, A global climatology of total ozone from Nimbus 7 total ozone mapping spectrometer, *J. Geophys. Res.*, *90*, 7967–7976, 1985.

Chandra, S., and R. S. Stolarski, Recent trends in the stratospheric total ozone: Implications of dynamical and El Chicon perturbations, *Geophys. Res. Lett.*, *18*, 2277–2280, 1991.

Chelliah, M., The global climate for June–August 1989: A season of near normal conditions in the tropical Pacific, *J. Clim.*, *3*, 138–162, 1990.

Hasebe, F., A global analysis of the fluctuations in total ozone, II, Non-stationary annual oscillation, quasi-biennial oscillation, and long-term variations in total ozone, *J. Meteorol. Soc. Jpn*, *58*, 104–117, 1980.

Hasebe, F., Dynamical response of the tropical total ozone to sea surface temperature changes, *J. Atmos. Sci.*, *50*, 345–356, 1993.

Herman, J. R., R. Hudson, R. McPeters, R. Stolarski, Z. Ahmad, X.-Y. Gu, S. Taylor, and C. Wellemeyer, A new self-calibration method applied to TOMS and SBUV backscattered ultraviolet data to determine long-term global ozone change, *J. Geophys. Res.*, *96*, 7531–7545, 1991.

Hilsenrath, E., and B. M. Schlesinger, Total ozone seasonal and interannual variations derived from the 7-year Nimbus 4 BUV dataset, *J. Geophys. Res.*, *86*, 12,087–12,096, 1981.

Kalnay, E., et al., The NCEP/NCAR 40-year reanalysis project, *Bull. Am. Meteorol. Soc.*, *77*, 437–471, 1996.

Komhyr, W. D., S. J. Oltmans, and R. D. Grass, Atmospheric ozone at south pole, Antarctica, in 1986, *J. Geophys. Res.*, *93*, 5167–5184, 1988.

Labitzke, K., and H. van Loon, The spatial distribution of the association between total ozone and the 11-year solar cycle, *Geophys. Res. Lett.*, *19*, 401–403, 1992.

Lait, L. R., R. Schoeberl, and P. A. Newman, Quasi-biennial modula-

tion of the Antarctic ozone depletion, *J. Geophys. Res.*, *94*, 11,559–11,571, 1989.

Randel, W. J., and J. B. Cobb, Coherent variations of monthly mean total ozone and lower stratospheric temperature, *J. Geophys. Res.*, *99*, 5433–5447, 1994.

Schubert, S. D., and M.-J. Munteanu, An analysis of tropopause pressure and total ozone correlations, *Mon. Weather Rev.*, *116*, 569–582, 1988.

Shiotani, M., Annual, quasi biennial, and El Niño-Southern Oscillation (ENSO) timescale variations in equatorial total ozone, *J. Geophys. Res.*, *97*, 7625–7633, 1992.

Stephenson, D. B., and J.-F. Royer, Low-frequency variability of total ozone mapping spectrometer and general circulation model total ozone stationary waves associated with the El Niño-Southern Oscillation for the period 1979–1988, *J. Geophys. Res.*, *100*, 7337–7346, 1995.

Tolson, R. H., Spatial and temporal variations of monthly mean total columnar ozone derived from 7 years of BUV data, *J. Geophys. Res.*, *86*, 7312–7330, 1981.

Trenberth, K. E., Signal versus noise in the Southern Oscillation, *Mon. Weather Rev.*, *112*, 326–332, 1984.

Zerefos, C. S., H. van Loon, and C. Repapis, Possible evidence of the Southern Oscillation in total ozone at Arosa, *Arch. Meteorol. Geophys. Bioklimatol., Ser. A*, *31*, 231–235, 1982.

Zerefos, C. S., A. F. Bais, I. C. Ziomas, and R. D. Bojkov, On the relative importance of quasi-biennial oscillation and El Niño-Southern Oscillation in the revised Dobson total ozone records, *J. Geophys. Res.*, *97*, 10,135–10,144, 1992.

M. T. Kayano, Instituto Nacional de Pesquisas Espaciais, Avenida dos Astronautas 1758, C.P. 515, 12201-970 São José dos Campos, Brazil. (e-mail: mary@met.inpe.br)

(Received March 4, 1997; revised August 8, 1997;
accepted August 20, 1997.)